Journal of Hydrology X 31 (2026) 100231

Contents lists available at ScienceDirect

Journal of Hydrology X

journal homepage: www.sciencedirect.com/journal/journal-of-hydrology-x

Letter

Multivariate design storms reveal misrepresentation of flood hazard by traditional approaches

Tabea Cache [a,b,*], Hannes Müller-Thomy [c], Christian Onof [d], Simon M. Papalexiou [e], Nadav Peleg [a,b]

[a] Institute of Earth Surface Dynamics, University of Lausanne, Lausanne, Switzerland
[b] Expertise Center for Climate Extremes, University of Lausanne, Lausanne, Switzerland
[c] Leichtweiß Institute for Hydraulic Engineering and Water Resources, Division of Hydrology and River Basin Management, Technische Universität Braunschweig, Brunswick, Germany
[d] Department of Civil and Environmental Engineering, Imperial College London, London, UK
[e] Institute for Global Water Security, Hamburg University of Technology, Germany

ARTICLE INFO

C. Wasko

Dataset link: https://www.meteoswiss.admin.ch/services-and-publications/applications/measurement-values.html, https://www.swisstopo.admin.ch/en/height-model-swissalti3d, https://www.swisstopo.admin.ch/en/landscape-model-swissbuildings3d-2-0

Keywords:
Design storms
Extreme precipitation
Joint return periods
Multivariate analysis
Urban flood hazard
Risk

ABSTRACT

Design storms are widely used in hydraulic engineering to represent extreme precipitation and assess flood risk. Commonly used block-method design storms, such as Euler Type II, assign a single return period across all temporal scales of an event, neglecting dependencies in rainfall intensity across durations. This simplification may lead to unrealistic event representations. Here, we compare flood hazard from a traditional Euler Type II storm with storms generated using the multivariate REALISTIC framework, which accounts for joint return periods across durations. Using Zurich as a case study, we simulate 3-hour 100-year events and evaluate the resulting flood hazard with a hydrodynamic model. Results show that flood hazard is highly sensitive to the underlying intensity-duration profile. The block-method storm produces substantially higher flood depths and intensities than events whose profiles are consistent with observed joint return periods, which often result in limited flooding. These findings suggest that traditional design storms provide an incomplete estimation of flood hazard and highlight the need for multivariate approaches to support more robust risk assessments.

Main

1.1. Traditional block-method design storms: an oversimplified representation of extreme precipitation events?

The design of hydraulic structures requires representative precipitation scenarios, so-called design storms, to estimate the likelihood of flood hazard and the risk associated with the structure's failure. Design storms are usually described by a small set of event statistics, such as event duration and return period associated with total precipitation volume. These statistics are usually fixed by national engineering guidelines. Design storms provide a simple yet attractive tool for risk assessment as they translate complex information into a single precipitation event. However, the return period assigned to a precipitation event depends on the aggregation duration (or window size) used to characterize it (Willems, 2000). A bivariate frequency analysis where a single return period-duration pair is considered can therefore provide an incomplete assessment of the probability of occurrence of a flood event and an inappropriate estimation of the risk.

Block-methods are widely used to construct design storms. They adopt the return period of the total precipitation volume (i.e., the return period associated with the precipitation aggregating moving window size equal to the event's duration) for all sizes of aggregating moving window within the event (e.g., Peleg et al., 2024). This method thereby ignores dependencies between precipitation intensity across different aggregating window sizes. Additionally, the return period of the complete rainfall profile does not directly follow from the return periods of its individual characteristics (Section 1.3). A related approach is used in the SCS/NRCS design storms, which prescribe a standardized 24-hour temporal pattern for a given precipitation volume (NRCS, 2021). Although the two approaches differ in how the temporal

* Corresponding author at: Institute of Earth Surface Dynamics, University of Lausanne, Lausanne, Switzerland.
E-mail address: tabea.cache@unil.ch (T. Cache).

https://doi.org/10.1016/j.hydroa.2026.100231
Received 18 September 2026; Accepted 24 September 2026
Available online 9 October 2026
2589-9155/© 2026 The Authors. Published by Elsevier B.V. This is an open access article under the CC BY license (http://creativecommons.org/licenses/by/4.0/).

rainfall profile is constructed, they share the underlying concept of concentrating rainfall volumes associated with a given return period within a single event. The main limitation of traditional design storms thus arises primarily from assumptions about intra-event joint probabilities, with additional effects from time series construction artifacts. Some studies have addressed this main shortcoming through multivariate analysis (Grimaldi and Serinaldi, 2006; Vandenberghe et al., 2010). More recently, Cache et al. (2025) have presented a stochastic design storm generator that accounts for the joint return period across multiple aggregating moving window sizes. While Cache et al. (2025) have studied the differences in precipitation properties, the hydraulic implications of the novel multivariate design storms remain unexplored. Considering the complex non-linear response of runoff to precipitation, it is crucial to assess whether differences in the joint return period of these storms translate into differences in simulated runoff response and flood hazard.

Here, we compare flood hazard for storms from traditional block-methods and for storms generated in a multivariate framework. For the block-method case, we adopt the Euler Type II design storm that is widely used in European guidelines. For the multivariate design storms, we use the stochastic generator REALISTIC from Cache (2025). We use the weighted cellular automata 2D model WCADv2 implemented in CADDIES-caflood (Guidolin et al., 2016) to simulate the runoff and the related flood hazard maps. This inundation model uses simple and parallelized transition rules for water transfer throughout the computation domain, allowing for fast flood modeling, and is broadly used for urban surface water flood modeling (Liu et al., 2018; Wang et al., 2019; Webber et al., 2018).

We choose Zurich as a case study and set the storm duration and total precipitation return period to respectively 3 h and 100-year, which corresponds to a total precipitation volume of 64.3 mm (Fig. 1). In the case of the Euler Type II design storm, the event is constrained in its precipitation duration and return period for all sizes of aggregating windows. In the case of the REALISTIC design storms, only the precipitation duration and the return period of the maximum size of the aggregating window are constrained (Fig. 1). This gives an infinite possibility of intensity-duration (ID) profiles. We simulate 100,000 profiles using the REALISTIC design storm model and then select three events from the simulation set with differing ID profiles (see the selection methodology in Section 2.3), representative of the range of possible profiles; (i) a lower contour profile with minimum return periods on aggregating window sizes smaller than the maximum size, (ii) the prevailing profile (i.e. a profile representative of the most probable 3 h 100-year event), and (iii) an upper contour profile with maximum return periods on aggregating window sizes smaller than the maximum size (Fig. 1). We also select one observed ID profile. We use these profiles as forcing for the CADDIES-caflood hydrodynamic model (Section 2.4) to analyze the differences in flood hazard.

1.2. Alternative design storms and their flood hazard implications

The flood hazard varies greatly depending on the ID profile of the 3-h 100-year events (Fig. 2, 3 and S2). Fig. 2 shows the maximum flood depth, maximum flood intensity (defined as the product of flood depth and velocity), and the flood hazard category affecting buildings (based on the maximum flood depth at each building) for Euler Type II and the prevailing REALISTIC design storm. Fig. 3 shows the relative differences in hazardous areas (defined as the maximum between flood depth and flood intensity) and in hazard levels affecting buildings between the traditional block-method (Euler Type II) event and the selection of events from the REALISTIC design storm model.

Flood depth is commonly used to estimate building damage and economic losses (Huizinga et al., 2017). While several areas of the city center are flooded under the Euler Type II event, almost no flooding occurs under the prevailing REALISTIC design storm (Fig. 2) for the same hazard (i.e., return period) level. Consequently, almost a third (31.8%) of the buildings are exposed to floodwater (i.e., depths above 0.1 m) in the former event, and this proportion falls to 1.7% in the latter event (Fig. 3). Hazard levels affecting flood-exposed buildings also vary considerably, with 4.4% of exposed buildings experiencing 'very high' hazard levels (i.e., flood depths above 2 m) under Euler Type II, whereas none do under the prevailing REALISTIC profile (Fig. 2). In terms of estimated economic losses due to damage to buildings, the Euler Type II event leads to damage costs of 373 M CHF (Fig. S3). Damages from the prevailing REALISTIC design storm are estimated at only 16.8 M CHF, representing a 95.5% reduction in losses compared to the Euler Type II design storm (Fig. S3).

Flood intensity is relevant for assessing risks to people and vehicles, as the shear force of flowing water strongly affects their stability in floodwaters (Evans et al., 2024). Flood intensity maps show a similar pattern to the flood depth maps, with several areas of the city center experiencing hazardous flood intensities under the Euler Type II scenario, whereas such conditions are nearly absent for the prevailing REALISTIC design storm (Fig. 2). In fact, one fifth (20.1%) of the city center reaches hazardous intensity levels in the Euler Type II case, while almost the entire area remains below hazardous thresholds in the prevailing REALISTIC profile.

Overall, the difference in flood hazard is particularly noticeable between Euler Type II and the prevailing REALISTIC profile, with a reduction in hazardous areas reaching 100% and a reduction in buildings exposed to floodwater reaching 100% for all categories except for the 'low hazard' category, where the reduction is equal to 92%. Similar trends are observed when comparing the traditional block-method design storm with other REALISTIC profiles (Fig. 3). Namely, the differences with the lower contour profile are almost identical to the ones from the prevailing profile, except that the reductions in buildings exposed to floodwater reach 100% for all categories. Consequently, this event is associated with no economic losses due to damage to buildings. The observed event has slightly lower, yet still substantial, differences in flood hazard and estimated flood risk. This translates to 60.8% of the buildings identified as exposed under the Euler Type II case remaining exposed under the observed event, and to a 68.7% reduction in economic losses. The former reduction is primarily driven by a decrease in the number of buildings in the 'medium' to 'very high' hazard categories. Differences are more pronounced for hazardous areas, with only 2.6% of the city center experiencing hazardous flood intensities, corresponding to an 86.8% reduction relative to the Euler Type II case. Lastly, although the upper contour most closely resembles the traditional block-method design storm and exhibits the highest peak intensity among simulated REALISTIC events, it does not reach the hazard level of the Euler Type II design storm. Hazardous areas, exposed buildings, and associated economic losses are reduced by 34.6%, 13.6%, and 18.4%, respectively. These differences are even larger for the 'very high' hazard category, with reductions of 76.6% in hazardous areas and 68.4% in exposed buildings.

1.3. Concluding remarks: flood risk overestimation by traditional design storms

All REALISTIC precipitation profiles and the observed profile used in the hydrodynamic simulations produce lower flood hazard than the Euler Type II event, even for the upper contour profile. Although all selected events share the same return period on the critical duration and are constructed using a consistent hyetograph methodology, they result in different flood depths and flood velocities. Consequently, all selected REALISTIC profiles and the observed profile exhibit lower flood risk, measured as the economic impact on buildings, than the Euler Type II event. These results demonstrate that traditional and commonly used block-method design storms provide an incomplete assessment of flood hazard and, consequently, an inappropriate estimation of flood risk.

Other characteristics of precipitation events may further influence flood hazard, such as the spatial distribution of rainfall (Baer et al.,

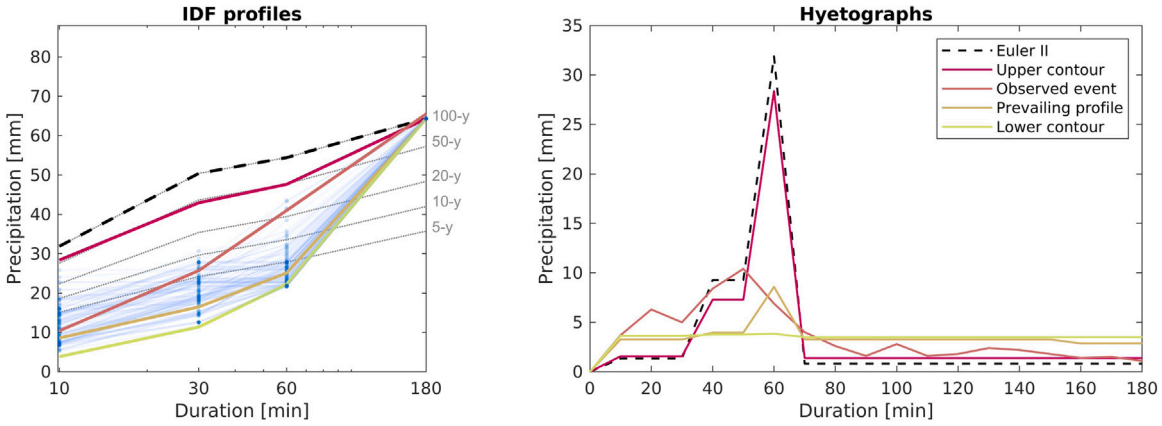


Fig. 1. Intensity-duration profiles (left) and precipitation time series (right) of the 100-year Euler Type II design storm, events simulated using the REALISTIC storm model, and an observed ID profile. The transparent blue lines in the left figure show possible realizations of the REALISTIC storm model, with a sample size of 100.

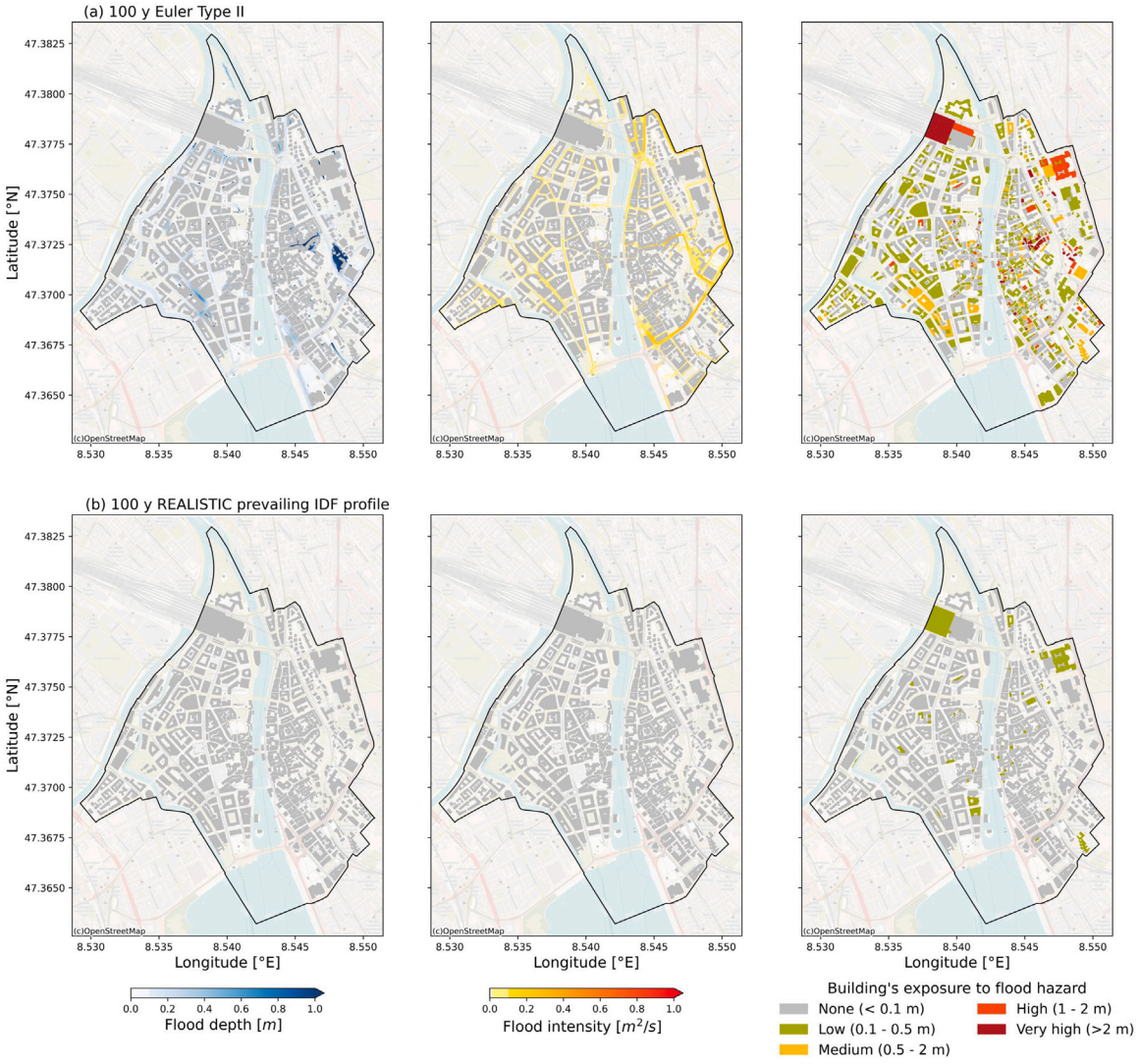


Fig. 2. Flood depth maps (left), flood intensity maps (center), and buildings exposed to flood hazard (right) in Zurich for (a) the 100-year Euler Type II design storm (top) and (b) the 100-year REALISTIC prevailing ID profile (bottom). The black line shows the contour of the study area.

2026; Müller and Haberlandt, 2018; Ochoa-Rodriguez et al., 2015; Peleg et al., 2017) or the shape of the hyetograph (Pritsis et al., 2024, Appendix S1) and are not considered in our analysis. In fact, the temporal structure of all precipitation events follows Euler Type II design storm construction guidelines (i.e., for converting ID profiles into hyetographs), which remains a simplification. Additionally, the

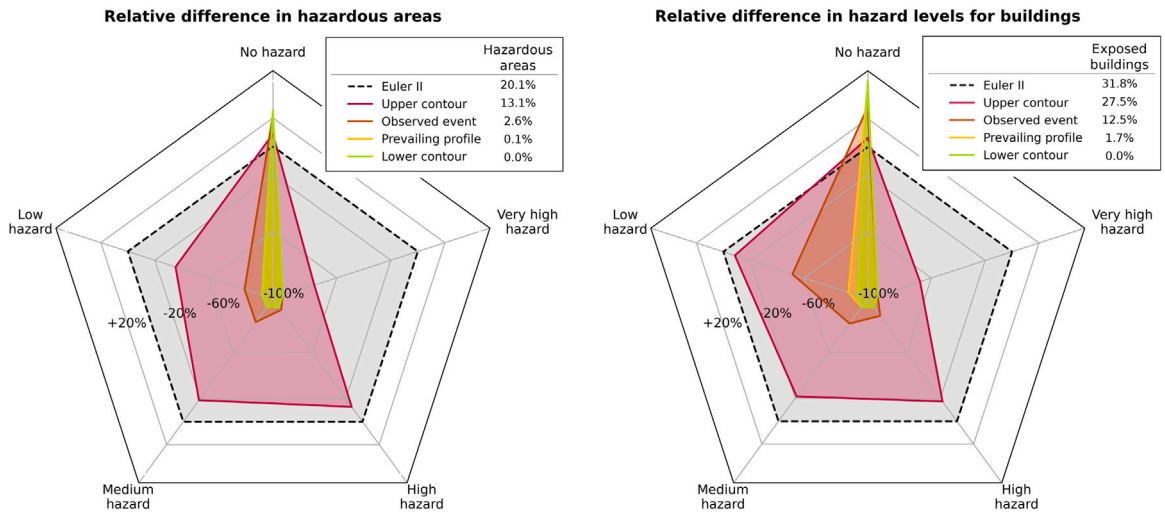


Fig. 3. Relative difference in hazard levels for buildings (left) and hazardous areas (right) between the 100-year Euler Type II design storm and the four events simulated using the REALISTIC storm model. The hazard categories for hazardous areas are defined based on the flood intensity, while those for buildings are defined solely based on the flood depth.

use of return period assumes that the observations are independent and identically distributed (Serinaldi, 2015), which may not hold in the multivariate frequency framework. While the total precipitation volume may correspond to a 100-year return period, its occurrence together with the temporal structure imposed by the block-method, implying the joint occurrence of multiple 100-year intensities within a single event, does not itself have a 100-year probability. Similar observations hold for the storms simulated in the multivariate REALISTIC framework. Lastly, the estimation of hazard and risk, measured as replacement costs of damaged buildings, comprises multiple assumptions (see Section 1.3). The estimations are thus indicative only and should not be interpreted as actual hazard maps and economic losses for these events, but rather as a basis for comparative analysis.

A further assumption underlying traditional design storms is the equality between the design hyetograph return period and runoff return period. This is closely linked to the construction of block-method design storms, imposing the same return period across a range of durations. While this can be motivated by the rationale of accounting for the range of response times (NRCS, 2021), it neglects the complex non-linear response of runoff. Furthermore, given that the unique joint return period is not physically realistic (Cache et al., 2025), the resulting 'worst-case' scenario should not be interpreted as a true worst-case event, but rather as a statistically unlikely combination of extremes that cannot realistically occur as a single event. Additionally, pursuing the objective of a 'worst-case' scenario might be undesirable in certain situations, such as insurance premium estimation or trust in early warnings, for example. While previous studies have argued that the equality relation is not generally valid (Pilgrim and Cordery, 1975; Rogger et al., 2012; Viglione et al., 2009), the aim of this study is not to resolve the broader challenge of deterministic mapping from storm to flood-frequency estimates, but rather to investigate how the use of a design storm with realistic dependence between intra-event joint return periods can alter the resulting runoff and hydraulic response relative to a traditional design-storm approach.

Our analysis highlights the role of intra-event variability and the limitations of the univariate (or bivariate) framework adopted for the construction of traditional design storms. In particular, we demonstrate the effect of joint return periods within precipitation events on the flood hazard component of flood risk assessments. As a result, the probability associated with the full temporal structure of traditional design storms is not consistent with their nominal return period. Accounting for the joint return periods of precipitation is essential for more robust flood risk assessments.

Although our simulations were conducted for Zurich and for a 3-h 100-year event, the main conclusion is likely transferable beyond this specific case. Because the limitations of the Euler Type II approach stem from its simplified representation of intra-event rainfall structure, rather than from local climate alone, we expect similar implications for flood hazard assessment in other catchments and cities, and across other relevant event durations and return periods. Although we specifically evaluated the Euler Type II design storm, the underlying issue is not unique to this method and likely applies to block-based design-storm approaches more generally, wherever a single return period is imposed across temporal scales within an event. Furthermore, considering the varying flood hazards obtained for the different events, the results emphasize the need to incorporate multiple design storm scenarios for robust risk assessment.

Stochastic uncertainty is a major source of uncertainty in flood modeling (Chen et al., 2025; Nathan, 2025). While explicitly accounting for it is critical for characterizing the full range of possible flood responses, it is not typically part of current engineering practice and requires a large number of simulations. Here, we consider an approach that remains comparable in scale to current engineering practice. The REALISTIC model can, however, be used to account for this uncertainty through ensemble simulations, but such an analysis is beyond the scope of the present study. Furthermore, while the present study proposes a method for identifying a prevalent storm, the question of which storm, or set of storms, is most representative remains open and is likely to depend on the applications and the aspects of uncertainty that need to be represented. Although the prevalent storm may be interpreted as the 'most probable' event here, the minimum–maximum envelope (represented by the lower and upper contours) may also provide important information by capturing the range of plausible flood responses, from best- to worst-case scenarios.

Methods

2.1. Data

We used the city of Zurich (Switzerland) as a case study. 10-minute precipitation data were obtained from MeteoSwiss for the stations of Zurich Affoltern, Fluntern, and Kloten over the period 1981–2022, and processed as described in Cache et al. (2025). The elevation data were extracted from the swissALTI3D product from swisstopo, at 2 m resolution, and the building footprints were extracted from the swissBUILIDNGS3D 2.0 product. The area for hydrodynamic modeling

was determined after delimitation of the catchments influencing pluvial flooding in the city of Zurich (Fig. S1), and we restricted the area for analysis of the results at the municipal district-level of Kreis 1.

2.2. The REALISTIC design storm model

The REALISTIC design storm model was used to simulate events that reproduce the joint return periods of observed precipitation in Zurich. Here, we provide a brief description of the model and refer the reader to Cache et al. (2025) for a full description.

First, the REALISTIC design storm model extracts the maximum precipitation volumes aggregated over moving windows of different sizes for each recorded precipitation event. Moving window sizes are user-defined and were here set to 10 min, 30 min, 1 h, and 3 h for our case study, as those are commonly used to analyze and characterize convective precipitation events (e.g. Villalobos Herrera et al., 2024). The duration of the design events is set to 3 h, as this is a typical duration of a design storm for urban areas.

The multivariate relationship between precipitation volumes over the 10-min to 3-h durations is then modeled using a copula. Let $\mathbf{X} = \{X_d\}$, where $d \in \{10, 30, 60, 180\}$ represents the vector of precipitation volumes corresponding to durations d. According to Sklar's theorem (Sklar, 1959), the multivariate distribution $F(\mathbf{X})$ can be decomposed into marginal distributions F_d and a copula C describing their dependence. After transforming the variables to uniform margins $u_d = F_d(X_d)$, by ranking the precipitation volumes and normalizing the ranks, the joint distribution is written as:

$$F(x_{10}, x_{30}, x_{60}, x_{180}) = C(u_{10}, u_{30}, u_{60}, u_{180}), \tag{1}$$

with

$$C(u_{10}, u_{30}, u_{60}, u_{180}) = F\{F_{10}^{-1}(u_{10}), \dots, F_{180}^{-1}(u_{180})\}. \tag{2}$$

Using the chain rule, the joint density can be written as:

$$f(x_{d_1}, \dots, x_{d_n}) = c_{d_1,\dots,d_n}\{F_{d_1}(x_{d_1}), \dots, F_{d_n}(x_{d_n})\} \prod_{i=1}^{n} f_{d_i}(x_{d_i}), \tag{3}$$

and can also be factorized into conditional densities.

The model adopts a canonical vine (C-vine) copula (Bedford and Cooke, 2002), where the joint density is expressed as a product of marginal densities and successive pair-copulas. The ordering of variables is determined from the dependence strength, so that the variables' position in the vine is ranked from strongest to weakest dependence.

The copula is estimated using non-parametric estimators of the pair-copula and inverse marginal cumulative distribution functions. Sampling from the copula follows the algorithm of Aas et al. (2009), where dependent uniform variables are generated through successive application of the pair-copula, which are then converted to precipitation volumes using the inverse marginal distributions. The same framework allows conditional sampling by fixing a return period at a given duration. The corresponding uniform variable is obtained from the marginal distribution, and the remaining variables are simulated conditionally using the vine structure. Similar to random sampling, the uniform variables are then converted to precipitation volumes using the inverse marginal distributions.

To enforce physical consistency, sampled volumes $\tilde{X}_d$ are corrected using the following relation:

$$\tilde{X'}_{d_i} = \begin{cases} \tilde{X}_{d_i}, & \text{if } d_i = 10 \\ \max\{\tilde{X'}_{d_{i-1}}, \tilde{X}_{d_i}\}, & \text{if } d_i > 10 \end{cases} \tag{4}$$

where $i \in \{1, 2, 3, 4\}$ and $(d_1, d_2, d_3, d_4) = (10, 30, 60, 180)$.

These precipitation volumes over the selected aggregation window size constitute the ID profiles of the simulated events.

The model can then generate hyetographs based on the ID profiles, either using a cascade model or following Euler Type II design storm construction guidelines. The second option is adopted here, to isolate the impact of ID profiles, without accounting for the variability in hyetograph shape, and to align with local guidelines (VSA, 2023).

2.3. Simulated precipitation events

Using the Euler Type II guidelines and the REALISTIC design storm model described above, we generated events with a 100-year return period on the 3 h duration. The former is commonly adopted for flood risk assessment (e.g., Kipfer et al., 2018). Intensity-duration-frequency (IDF) relationships of precipitation in Zurich were computed using the TENAX model (Marra et al., 2024), as described in Cache et al. (2025), leading to a 3-h 100-y precipitation volume of 64.3 mm (Fig. 1).

The Euler Type II design storm is commonly used in several European countries for engineering practices. It is constructed by first identifying the entire ID profile corresponding to a certain return period, here set to 100-year. Second, the precipitation intensities are split into 10-min resolution, sorted from largest to smallest value, and flipped at the first one-third of the sorted data (DWA-A 118, 2006).

The REALISTIC design storms are generated using conditional sampling from the vine copula, with the constraint of a 100-y precipitation volume on the 3-h duration. In order to select representative profiles, we first generated 100,000 samples. We then select (i) a lower contour, (ii) a prevailing profile, and (iii) an upper contour. The lower and upper contours are defined by selecting ID profiles that minimize and maximize precipitation volumes over durations shorter than 3 h, giving greater weight to the minimization, respectively maximization, of precipitation volumes over shorter durations. The selection process of the prevailing profile is slightly more complex. First, we define tolerance window sizes for each duration. These windows are computed relative to the precipitation volumes across durations, using a tolerance of 5 years around the 100-year ID profile. In practice, the window size at each duration is defined as the difference in precipitation volumes between the 105-year and the 95-year ID profiles. This results in non-symmetrical tolerance windows, since the difference between the 100-year and 105-year profiles is smaller than that between the 100-year and 95-year profiles. Next, for each generated ID profile, we define its tolerance window by adding and subtracting these differences from the corresponding precipitation volumes. We then count how many generated profiles fall within the tolerance windows at all durations. Finally, the prevailing profile is defined as the profile with the highest count. It is worth noting that, when applying this procedure to the Euler Type II design storm and comparing with the 100,000 generated samples, none of the generated samples fall within its tolerance windows across all durations. Furthermore, as the intensity-duration profiles are randomly generated, the representative profiles selected could change with a different set of simulations.

We also extracted an observed event whose precipitation volume at the 3-h duration is as close as possible to the 100-year value, i.e., 64.3 mm. The event that best meets this criterion is shown by the orange line in Fig. 1, with a 3-hour precipitation volume of 65.5 mm.

After generating the REALISTIC design storms and selecting the observed event ID profiles, we computed their hyetographs by following the Euler Type II construction guidelines described above.

2.4. Hydrodynamic simulations

We used these profiles as forcing of the cellular automata model WCADv2, implemented in CADDIES-caflood (Guidolin et al., 2016), assuming dry antecedent conditions, and saved the flood depth and flood velocity maps every 3 min of simulation time. In Switzerland, urban drainage is normally designed for a 5- to 10-y event (Kipfer et al., 2018; VSA, 2023). We therefore adopted a 33.6 mm h^{-1} infiltration rate in WCADv2, which corresponds to the 10-y 1-h precipitation volume in Zurich (see Fig. 1). This is a simplified method to account for the urban drainage network. As such, the flood modeling results should be interpreted as indicative rather than as detailed flood hazard assessments for the city of Zurich.

Table 1
Hazard categories following guidelines from SIA (2020).

Hazard category	Flood depth h [m]	Flood intensity $v \cdot h$ [m^2 s^{-1}]
None	$h < 0.1$	$v \cdot h < 0.1$
Low	$0.1 \leq h \leq 0.5$	$0.1 \leq v \cdot h \leq 0.5$
Medium	$0.5 \leq h \leq 1$	$0.5 \leq v \cdot h \leq 1$
High	$1 \leq h \leq 2$	$1 \leq v \cdot h \leq 2$
Very high	$h \geq 2$	$v \cdot h \geq 2$

2.5. Hazard categories

After simulating the flood maps, we analyzed flood depth, flood intensities, and flood hazard categories (Figs. 2 and 3). We adopted the definition of flood intensity from the Swiss construction standards (SIA, 2020), i.e., the product of flood depth h and flood velocity v, and adapted their hazard categories. In fact, we used the thresholds from SIA (2020) but added the distinction between 'high' and 'very high' hazard (Table 1).

We used these thresholds to compute the hazard categories to which buildings are exposed. To do so, we first extracted the buildings' footprint geometries from swissBUILDINGS3D. We then spatially joined the flood depth raster and building geometries. The hazard category to which each building is exposed was finally defined by extracting the maximum flood depth touching the building, and following the thresholds in Table 1.

We also computed hazard categories across the study area to identify hazardous zones, which are important for assessing flood risk to people and vehicles. To do this, we first excluded building footprints and the river from the analysis area. We then classified flood depth and flood intensity based on the thresholds in Table 1. Finally, we defined the flood hazard map as the maximum hazard category derived from either flood depth or flood intensity.

2.6. Economic losses

Finally, we calculated the impact of each event as the economic losses due to damage to buildings. This requires three components: hazard, exposure, and vulnerability. The flood depth maps constitute the hazard component, and exposure was measured as the replacement costs of the buildings. These costs were calculated for each building as its footprint area multiplied by a unit repair cost, assumed to be 4000 CHF m^{-2} for Zurich (UBS, 2024). For the vulnerability component, we used the impact function developed by the Joint Research Center for residential buildings in Europe (see Fig. S3a, Huizinga et al., 2017). By linking the maximum water depth each building is exposed to with the corresponding damage ratio, we estimated the economic losses for each building (e.g., Fig. S3).

Code availability

The REALISTIC design storm model is freely available for non-commercial use and can be accessed from: https://zenodo.org/records/15119797.

Declaration of competing interest

The authors declare that they have no known competing financial interests or personal relationships that could have appeared to influence the work reported in this paper.

Acknowledgments

TC and NP were supported by the Swiss National Science Foundation (SNSF), Grant 194649 ("Rainfall and floods in future cities").

Appendix A. Supplementary data

Supplementary material related to this article can be found online at https://doi.org/10.1016/j.hydroa.2026.100231.

Data availability

Precipitation data were obtained from MeteoSwiss: https://www.meteoswiss.admin.ch/services-and-publications/applications/measurement-values.html. The elevation data from the swissALTI3D product are available at: https://www.swisstopo.admin.ch/en/height-model-swissalti3d, and the building footprints are extracted from the swissBUILIDNGS3D 2.0 product, which can be accessed from: https://www.swisstopo.admin.ch/en/landscape-model-swissbuildings3d-2-0.

References

Aas, K., Czado, C., Frigessi, A., Bakken, H., 2009. Pair-copula constructions of multiple dependence. Insurance Math. Econom. 44, 182–198. http://dx.doi.org/10.1016/j.insmatheco.2007.02.001.

Baer, J.A., Sebastian, A., Grimley, L.E., Doss-Gollin, J., Wright, D.B., Hussain, M.A., Webber, M.K., 2026. Neglecting spatiotemporal rainfall variability misrepresents flood hazard and risk. npj Nat. Hazards http://dx.doi.org/10.1038/s44304-026-00208-5.

Bedford, T., Cooke, R.M., 2002. Vines - a new graphical model for dependent random variables. Ann. Statist. 30, 1031–1068. http://dx.doi.org/10.1214/aos/1031689016.

Cache, T., 2025. REALISTIC design storm model. http://dx.doi.org/10.5281/zenodo.15119797, Zenodo.

Cache, T., Bevacqua, E., Zscheischler, J., Müller-Thomy, H., Peleg, N., 2025. Simulating realistic design storms: A joint return period approach. Water Resour. Res. 61 (7), e2024WR039739. http://dx.doi.org/10.1029/2024WR039739.

Chen, M., Mahto, S.S., He, X., Jun, C., Paschalis, A., Peleg, N., Mascaro, G., Fatichi, S., 2025. Record-breaking rainfall: a stochastic approach for its prediction. npj Nat. Hazards 2, 98. http://dx.doi.org/10.1038/s44304-025-00148-6.

DWA-A 118, 2006. DWA-A 118: Hydraulische Bemessung und Nachweis von Entwässerungssystemen. Deutsche Vereinigung für Wasserwirtschaft, Abwasser und Abfall e.V. (DWA), Hennef.

Evans, B., Lam, A., West, C., Ahmadian, R., Djordjević, S., Chen, A., Pregnolato, M., 2024. A combined stability function to quantify flood risks to pedestrians and vehicle occupants. Sci. Total Environ. 908, 168237. http://dx.doi.org/10.1016/j.scitotenv.2023.168237.

Grimaldi, S., Serinaldi, F., 2006. Design hyetograph analysis with 3-copula function. Hydrol. Sci. J. 51, 223–238. http://dx.doi.org/10.1623/hysj.51.2.223.

Guidolin, M., Chen, A.S., Ghimire, B., Keedwell, E.C., Djordjević, S., Savić, D.A., 2016. A weighted cellular automata 2D inundation model for rapid flood analysis. Environ. Model. Softw. 84, 378–394. http://dx.doi.org/10.1016/J.ENVSOFT.2016.07.008.

Huizinga, J., Moel, H.D., Szewczyk, W., 2017. Global Flood Depth-Damage Functions: Methodology and the Database with Guidelines. Technical Report KJ-NA-28552-EN-N, Publications Office of the European Union, Joint Research Centre, Luxembourg (Luxembourg), http://dx.doi.org/10.2760/16510.

Kipfer, A., Berger, C., Mani, P., Hulliger, R., Caduff, U., Dobmann, J., Gsteiger, P., Pauli, M., Schneider, M., 2018. Gefährdungskarte Oberflächenabfluss. Technical Report, geo7 AG, Bern, Switzerland, Prepared for Bundesamt für Umwelt (BAFU), Schweizerischer Versicherungsverband (SVV), and Vereinigung Kantonaler Gebäudeversicherungen (VKG).

Liu, H., Wang, Y., Zhang, C., Chen, A.S., Fu, G., 2018. Assessing real options in urban surface water flood risk management under climate change. Nat. Hazards 94 (1), 1–18. http://dx.doi.org/10.1007/s11069-018-3349-1.

Marra, F., Koukoula, M., Canale, A., Peleg, N., 2024. Predicting extreme sub-hourly precipitation intensification based on temperature shifts. Hydrol. Earth Syst. Sci. 28 (2), 375–389. http://dx.doi.org/10.5194/hess-28-375-2024.

Müller, H., Haberlandt, U., 2018. Temporal rainfall disaggregation using a multiplicative cascade model for spatial application in urban hydrology. J. Hydrol. 556, 847–864. http://dx.doi.org/10.1016/j.jhydrol.2016.01.031.

Nathan, R., 2025. Improving event-based methods for modelling flood risk in a variable and non-stationary climate. Philos. Trans. R. Soc. A: Math. Phys. Eng. Sci. 383 (2302), 20240292. http://dx.doi.org/10.1098/rsta.2024.0292.

NRCS, 2021. Natural Resources Conservation Service National Engineering Handbook, second ed. United States Department of Agriculture.

Ochoa-Rodriguez, S., Wang, L.P., Gires, A., Pina, R.D., Reinoso-Rondinel, R., Bruni, G., Ichiba, A., Gaitan, S., Cristiano, E., van Assel, J., Kroll, S., Murlà-Tuyls, D., Tisserand, B., Schertzer, D., Tchiguirinskaia, I., Onof, C., Willems, P., ten Veldhuis, M.-C., 2015. Impact of spatial and temporal resolution of rainfall inputs on urban hydrodynamic modelling outputs: A multi-catchment investigation. J. Hydrol. 531, 389–407. http://dx.doi.org/10.1016/j.jhydrol.2015.05.035, Hydrologic Applications of Weather Radar.

Peleg, N., Blumensaat, F., Molnar, P., Fatichi, S., Burlando, P., 2017. Partitioning the impacts of spatial and climatological rainfall variability in urban drainage modeling. Hydrol. Earth Syst. Sci. 21 (3), 1559–1572. http://dx.doi.org/10.5194/hess-21-1559-2017.

Peleg, N., Wright, D.B., Fowler, H.J., Leitão, J.P., Sharma, A., Marra, F., 2024. A simple and robust approach for adapting design storms to assess climate-induced changes in flash flood hazard. Adv. Water Resour. 193, 104823. http://dx.doi.org/10.1016/j.advwatres.2024.104823.

Pilgrim, D.H., Cordery, I., 1975. Rainfall temporal patterns for design floods. J. Hydraul. Div. 101 (1), 81–95. http://dx.doi.org/10.1061/JYCEAJ.0004197.

Pritsis, S., Pons, V., Rokstad, M.M., Clemens-Meyer, F.H.L.R., Kleidorfer, M., Tscheikner-Gratl, F., 2024. The role of hyetograph shape and designer subjectivity in the design of an urban drainage system. Water Sci. Technol. 90 (3), 920–934. http://dx.doi.org/10.2166/wst.2024.261.

Rogger, M., Kohl, B., Pirkl, H., Viglione, A., Komma, J., Kirnbauer, R., Merz, R., Blöschl, G., 2012. Runoff models and flood frequency statistics for design flood estimation in Austria – Do they tell a consistent story? J. Hydrol. 456–457, 30–43. http://dx.doi.org/10.1016/j.jhydrol.2012.05.068.

Serinaldi, F., 2015. Dismissing return periods! Stoch. Environ. Res. Risk Assess. 29 (1), 1179–1189. http://dx.doi.org/10.1007/s00477-014-0916-1.

SIA, 2020. SIA 261.1. Einwirkungen auf Tragwerke - Ergänzende Festlegungen. Swiss Society of Engineers and Architects.

Sklar, A., 1959. Fonctions de répartition à n dimension et leurs marges. Institut Statistique de l'Université Paris, pp. 229–231.

UBS, 2024. Building a house: important facts and tips. URL https://www.ubs.com/ch/en/services/guide/mortgages-and-financing/articles/tips-for-building-a-house.html.

Vandenberghe, S., Verhoest, N.E., Buyse, E., Baets, B.D., 2010. A stochastic design rainfall generator based on copulas and mass curves. Hydrol. Earth Syst. Sci. 14, 2429–2442. http://dx.doi.org/10.5194/hess-14-2429-2010.

Viglione, A., Merz, R., Blöschl, G., 2009. On the role of the runoff coefficient in the mapping of rainfall to flood return periods. Hydrol. Earth Syst. Sci. 13 (5), 577–593. http://dx.doi.org/10.5194/hess-13-577-2009.

Villalobos Herrera, R., Blenkinsop, S., Guerreiro, S.B., Dale, M., Faulkner, D., Fowler, H.J., 2024. Towards new design rainfall profiles for the United Kingdom. J. Flood Risk Manag. 17, e12958. http://dx.doi.org/10.1111/jfr3.12958.

VSA, 2023. Évaluation hydraulique dans l'évacuation des eaux des agglomérations - Vérification de systèmes d'évacuation des eaux et gestion du ruissellement de surface. Technical Report, VSA.

Wang, Y., Meng, F., Liu, H., Zhang, C., Fu, G., 2019. Assessing catchment scale flood resilience of urban areas using a grid cell based metric. Water Res. 163, 114852. http://dx.doi.org/10.1016/j.watres.2019.114852.

Webber, J.L., Fu, G., Butler, D., 2018. Rapid surface water intervention performance comparison for urban planning. Water Sci. Technol. 77 (8), 2084–2092. http://dx.doi.org/10.2166/wst.2018.122.

Willems, P., 2000. Compound intensity/duration/frequency-relationships of extreme precipitation for two seasons and two storm types. J. Hydrol. 233 (1–4), 189–205. http://dx.doi.org/10.1016/S0022-1694(00)00233-X.